



**HAL**  
open science

## Biological behaviors of mutant proinsulin contribute to the phenotypic spectrum of diabetes associated with insulin gene mutations

Heting Wang, Cécile Saint-Martin, Jialu Xu, Li Ding, Ruodan Wang, Wenli Feng, Ming Liu, Hua Shu, Zhenqian Fan, Leena Haataja, et al.

### ► To cite this version:

Heting Wang, Cécile Saint-Martin, Jialu Xu, Li Ding, Ruodan Wang, et al.. Biological behaviors of mutant proinsulin contribute to the phenotypic spectrum of diabetes associated with insulin gene mutations. *Molecular and Cellular Endocrinology*, 2020, 518, pp.111025 -. 10.1016/j.mce.2020.111025 . hal-03492514

**HAL Id: hal-03492514**

**<https://hal.science/hal-03492514>**

Submitted on 21 Sep 2022

**HAL** is a multi-disciplinary open access archive for the deposit and dissemination of scientific research documents, whether they are published or not. The documents may come from teaching and research institutions in France or abroad, or from public or private research centers.

L'archive ouverte pluridisciplinaire **HAL**, est destinée au dépôt et à la diffusion de documents scientifiques de niveau recherche, publiés ou non, émanant des établissements d'enseignement et de recherche français ou étrangers, des laboratoires publics ou privés.



Distributed under a Creative Commons Attribution - NonCommercial 4.0 International License

1 **Biological Behaviors of Mutant Proinsulin Contribute to the Phenotypic Spectrum**  
2 **of Diabetes Associated with Insulin Gene Mutations**

3

4 Heting Wang<sup>a</sup>, Cécile Saint-Martin<sup>a,b</sup>, Jialu Xu<sup>a</sup>, Li Ding<sup>a</sup>, Ruodan Wang<sup>a</sup>, Wenli  
5 Feng<sup>a</sup>, Ming Liu<sup>a</sup>, Hua Shu<sup>a</sup>, Zhenqian Fan<sup>c</sup>, Leena Haataja<sup>d</sup>, Peter Arvan<sup>d</sup>, Christine  
6 Bellanné-Chantelot<sup>\* b</sup>, Jingqiu Cui<sup>\* a</sup>, Yumeng Huang<sup>\* a</sup>

7 <sup>a</sup>. Department of Endocrinology and Metabolism, Tianjin Medical University General  
8 Hospital, Tianjin, China.

9 <sup>b</sup>. Department of Genetics, Sorbonne University, Pitié-Salpêtrière Hospital,  
10 Assistance Publique-Hôpitaux de Paris, Paris, France

11 <sup>c</sup>. Department of Endocrinology and Metabolism, The Second Hospital of Tianjin  
12 Medical University, Tianjin, China.

13 <sup>d</sup>. Division of Metabolism, Endocrinology & Diabetes, University of Michigan Medical  
14 School, Ann Arbor, Michigan.

15

16 <sup>^</sup> these authors contribute equally

17 <sup>\*</sup> corresponding authors:

18 Yumeng Huang:

19 Email address: [huangyumengnc@126.com](mailto:huangyumengnc@126.com).

20 Address: Department of Endocrinology and Metabolism, Tianjin Medical University  
21 General Hospital, 154 Anshan road, Heping district, Tianjin 300052, China.

22

23 Jingqiu Cui:

24 Email address: [cuijingqiu@sina.com](mailto:cuijingqiu@sina.com)

25 Address: Department of Endocrinology and Metabolism, Tianjin Medical University

26 General Hospital, 154 Anshan road, Heping district, Tianjin 300052, China.

27

28 Christine Bellanné-Chantelot:

29 Email address: [christine.bellanne-chantelot@aphp.fr](mailto:christine.bellanne-chantelot@aphp.fr)

30 Address: Hôpital Pitié-Salpêtrière, Département de Génétique, 47-83 Bd de l'Hôpital,

31 75013 Paris, France

32

33

34

35

36

37

38

39

40

41

42

43

44

45 **Abstract**

46

47 Insulin gene mutation is the second most common cause of neonatal diabetes  
48 (NDM). It is also one of the genes involved in maturity-onset diabetes of the young  
49 (MODY). We aim to investigate molecular behaviors of different *INS* gene variants  
50 that may correlate with the clinical spectrum of diabetes phenotypes. In this study,  
51 we concentrated on two previously uncharacterized MODY-causing mutants,  
52 proinsulin-p.Gly44Arg [G(B20)R] and p.Pro52Leu [P(B28)L] (a novel mutant  
53 identified in one French family), and an NDM causing proinsulin-p.(Cys96Tyr)  
54 [C(A7)Y]. We find that these proinsulin mutants exhibit impaired oxidative folding  
55 in the endoplasmic reticulum (ER) with blocked ER export, ER stress, and apoptosis.  
56 Importantly, the proinsulin mutants formed abnormal intermolecular disulfide  
57 bonds that not only involved the mutant proinsulin, but also the co-expressed  
58 WT-proinsulin, forming misfolded disulfide-linked proinsulin complexes. This  
59 impaired the intracellular trafficking of WT-proinsulin and limited the production of  
60 bioactive mature insulin. Notably, although all three mutants presented with  
61 similar defects in folding, trafficking, and dominant negative behavior, the degrees  
62 of these defects appeared to be different. Specifically, compared to MODY mutants  
63 G(B20)R and P(B28)L that partially affected folding and trafficking of co-expressed  
64 WT-proinsulin, the NDM mutant C(A7)Y resulted in an almost complete blockade of  
65 the ER export of WT-proinsulin, decreasing insulin production, inducing more  
66 severe ER stress and apoptosis. We thus demonstrate that differences in cell

67 biological behaviors among different proinsulin mutants correlate with the  
68 spectrum of diabetes phenotypes caused by the different *INS* gene mutations.

69

70 **Keywords**

71 Neonatal diabetes mellitus; Maturity onset diabetes of the young; Proinsulin  
72 misfolding; ER stress; Dominant negative effect; Insulin gene mutations

73

74 **Abbreviations**

75	DLPC	Disulfide-linked proinsulin complexes
76	ER	Endoplasmic reticulum
77	EV	Empty vector
78	HMW	High molecular weight
79	INS	Insulin
80	MODY	Maturity onset diabetes of the young
81	NDM	Neonatal diabetes mellitus
82	WT	Wide type

83

84

85

86

87

88

89 **1. Introduction**

90

91 Upon delivery into the oxidized endoplasmic reticulum (ER) lumen, proinsulin (the  
92 insulin precursor) undergoes rapid oxidative folding, forming three highly conserved  
93 disulfide bonds (B7-A7, B19-A20, and A6-A11) (Liu, Weiss, Arunagiri et al., 2018, Sun,  
94 Cui, He et al., 2015). Proinsulin bearing its native disulfide bonds exits the ER to  
95 travel through the Golgi complex and immature secretory granules, where  
96 proinsulin begins to be processed by prohormone convertase 1/2 (PC1/2) and  
97 carboxypeptidase E (CPE), forming mature insulin. It has been long believed that  
98 proinsulin folding, intracellular trafficking, and processing occur very efficiently  
99 (Dodson and Steiner, 1998, Steiner, Cunningham, Spigelman et al., 1967); however,  
100 more recent genetic and biological evidence indicate that proinsulin folding in the  
101 ER is not as efficient as was previously thought. Under normal physiological  
102 conditions, up to 10-15% of newly synthesized proinsulin may form mispaired  
103 intramolecular and/or intermolecular disulfide bonds (Guo, Xiong, Witkowski et al.,  
104 2014, Liu, Lara-Lemus, Shan et al., 2012, Liu, Li, Cavener et al., 2005, Liu,  
105 Ramos-Castañeda and Arvan, 2003, Schuit, In't Veld and Pipeleers, 1988), and  
106 misfolded proinsulin may increase further when beta cells are forced to synthesize  
107 more proinsulin to compensate insulin resistance (Arunagiri, Haataja, Pottekat et al.,  
108 2019) or in beta cells with defective ER protein folding and export machinery (Zhu,  
109 Li, Xu et al., 2019, Jang, Pottekat, Poothong et al., 2019, Tsuchiya, Saito, Kadokura et  
110 al., 2018, Zito, Chin, Blais et al., 2010, Li, Itani, Haataja et al., 2019).

111

112 The pathological significance of misfolded proinsulin in the pathogenesis of diabetes

113 has been highlighted by the discovery of new diabetogenic insulin gene mutations  
114 (Colombo, Porzio, Liu et al., 2008,Stoy, Edghill, Flanagan et al., 2007). To date, about  
115 60 insulin gene variants have been identified in patients with monogenic diabetes  
116 (Liu, Sun, Cui et al., 2015,Liu, Hodish, Haataja et al., 2010,Weiss, 2009). More than  
117 half of these variants are predicted or experimentally confirmed to cause proinsulin  
118 misfolding in the ER (Liu et al., 2012,Park, Ye, Steiner et al., 2010,Liu, Haataja,  
119 Wright et al., 2010). Interestingly, the diabetes phenotypes caused by these variants  
120 range from severe insulin-deficient neonatal diabetes (NDM) to relative mild  
121 maturity onset diabetes of the young (MODY) (Stoy et al., 2007,Liu et al., 2015,Liu  
122 et al., 2010,Polak, Dechaume, Cavé et al., 2008,Edghill, Flanagan, Patch et al.,  
123 2008,Meur, Simon, Harun et al., 2010,Molven, Ringdal, NordbÅ, et al., 2008). The  
124 molecular mechanisms underlying the extent of this phenotypic spectrum of  
125 diabetes remain unclear.

126

127 In this study, we functionally characterized two new *INS* gene variants [G(B20)R and  
128 P(B28)L, identified in three French MODY patients with age of onset from 17 – 40  
129 years old] in comparison to the NDM proinsulin mutant C(A7)Y. We found that  
130 MODY mutants showed partial defects in their oxidative folding and ER export  
131 compared with the NDM mutant. All of the mutants formed disulfide-linked  
132 proinsulin complexes (DLPC) with WT-proinsulin, thus impairing WT-proinsulin ER  
133 export and decreasing mature insulin production, but the severity of the  
134 phenotypes varied, with C(A7) being most severe. Thus, cell biological defects

135 exhibited by mutant proinsulins appear to correlate with the clinical spectrum of  
136 diabetes phenotypes associated with different *INS* gene mutants.

137

## 138 **2. Material and Methods**

139

### 140 **2.1. Patients**

141 Three patients were recruited for genetic testing of monogenic diabetes. The  
142 biological collection of the Department of Genetics of Pitié-Salpêtrière Hospital has  
143 been declared to the Minister for research and the Director of the Regional Health  
144 Agency (biobank ID #DC2009-957). Patients signed an informed consent for the  
145 molecular diagnosis of their diabetes also indicating they approved to any research  
146 project performed in relation with their disease. Results of the genetic analyses are  
147 registered in a diagnosis database (CNIL certificate 16/02/2010-n°1412729). The  
148 study was done in agreement with the Declaration of Helsinki.

149

### 150 **2.2. Genetic analyses**

151 Targeted sequencing was performed based on a multiplex PCR assay  
152 (MODY-MASTR™ assay, Agilent) as previously described (Donath, Saint-Martin,  
153 Dubois-Laforgue et al., 2019). We used the sequence variant nomenclature  
154 recommendations (<http://varnomen.hgvs.org/>) for describing *INS* (NM\_000207.2)  
155 variants and classified them following the American College of Medical Genetics  
156 and Genomics (ACMG) guidelines (Richards, Aziz, Bale et al., 2015).



157

158 **2.3. Reagents and antibodies**

159 Lipofectamine 2000 and 4-12% NuPage gel were purchased from Invitrogen  
160 (Carlsbad, CA, USA). Protein phosphatase inhibitor was purchased from Beyotime  
161 Biotechnology (Beijing, China). Protein A-Agarose was from Santa Cruz  
162 Biotechnology (Dallas, TX, USA). Guinea pig anti-insulin (dilution: 1:2000) was from  
163 Merck Millipore (Billerica, MA, USA) and mouse anti-proinsulin antibody was from  
164 Novus Biologicals (Littleton, CO, USA). Rabbit anti-Hsp90 (dilution: 1:2000) antibody  
165 was from Assay designs (Ann Arbor, MI, USA). Rabbit anti-cleaved caspase 3  
166 antibody was from Cell Signalling Technology (Danvers, MA, USA). Annexin V with  
167 Alexa Fluor™ 555 conjugation, Goat anti-guinea pig IgG Alexa Fluor 555 and goat  
168 anti-rabbit IgG Alexa Fluor 435 was bought from Invitrogen (Carlsbad, CA, USA).  
169 Rabbit anti-Myc antibody was from Immunology Consultants Labs. Horseradish  
170 peroxidase–conjugated antibodies were from Jackson ImmunoResearch  
171 Laboratories (West Grove, PA, USA). Enhanced chemiluminescence Western blotting  
172 substrate was from Millipore (Billerica, MA, USA). Trans<sup>35S</sup> label and  
173 pure <sup>35S</sup>-methionine were from PerkinElmer (Waltham, MA, USA).

174

175 **2.4. Construction of plasmids encoding WT and mutant proinsulin**

176 The plasmids encoding human WT preproinsulin with or without Myc-tag or  
177 GFP-tag in the C-peptide were described as previously (Liu et al., 2012, Liu et al.,  
178 2010, Guo, Sun, Li et al., 2018). G(B20)R or P(B28)L mutations was introduced into

179 the constructs using the following primers: G(B20)R  
180 5'-TCTACCTAGTGTGCAGGGAACGAGGCTTCTTC-3', P(B28)L  
181 5'-CTTCTTCTACACACTCAAGACCCGCCGG-3', with the QuikChange site-directed  
182 mutagenesis kit (Stratagene, La Jolla, CA, USA). All mutations were confirmed by  
183 DNA sequencing in using primer 5'-CTGTGGATGCGCCTCCTGC-3'.

184

## 185 **2.5. Cell culture**

186 Human embryonic kidney 293T (293T) cells and INS1 rat insulinoma cells were  
187 purchased from ATCC (Manassas, VA, USA). 293T cells were cultured in Dulbecco's  
188 Modified Eagle Medium (DMEM) with 10% Fetal bovine serum (FBS), penicillin (100  
189 units/mL), and streptomycin (100 µg/mL). The INS1 cells were cultured in RPMI  
190 1640 supplemented with 10% FBS, 1 mM sodium pyruvate, 10 mM HEPES, and 0.05  
191 mM 2-mercaptoethanol (Sigma, St Louis, MO, USA). Mycoplasma detection and STR  
192 analysis were performed in these two cell lines.

193

## 194 **2.6. Cells transfection, <sup>35</sup>S-Met/Cys labeling, and immunoprecipitation**

195 293T cells were seeded into 12-well plates 24 hours before transfection to achieve  
196 70-90% cell confluent on the day of transfection. For each well, a total of 1 µg  
197 plasmid DNA was transfected using Lipofectamine 2000. At 48 hours post  
198 transfection, the cells were cultured with <sup>35</sup>S labeled amino acids and chased for the  
199 times indicated. The cells were washed once with PBS containing 20 mmol/L N-ethyl  
200 maleimide, then lysed in immunoprecipitation buffer [0.1M Tris-HCl 25mM (PH 7.0) ,

201 20mM EDTA 5mM (PH 8.0), 1M NaCl 100mM, Triton×-100 0.1%]. A proteinase  
202 inhibitor cocktail was added to cell lysates and chase media. Trichloroacetic acid  
203 (TCA)-precipitable counts were used to quantify and normalize the amount of  
204 total protein among samples. The samples were immunoprecipitated with  
205 anti-insulin at 4°C overnight. Anti-insulin immunoprecipitates were washed twice  
206 with immunoprecipitation buffer and then boiled in SDS sample buffer with or  
207 without 100 mM DTT for 5 minutes, and analyzed in tris-tricine-urea-SDS-PAGE or  
208 4-12% NuPage as indicated. Bands were quantified using ImageJ.

209

## 210 **2.7. Fully /Partially-reduced two-dimensional electrophoresis (2-DE)**

211 After 48 hours post transfection, 293T cells were lysed and resolved in 4-12%  
212 NuPage gel under non reducing condition. Fully-reduced 2-DE assay was carried out  
213 as following protocol: the gel was cut into six pieces, corresponding to the  
214 molecular weight of 6-14KD, 14-28KD, 28KD-38KD, 38KD-49KD, 49-98KD and  
215 98-198KD. The gel pieces were boiled in loading buffer containing 100mM DTT for 5  
216 minutes and run again in 4-12% NuPage gel. For Partially-reduced 2-DE assay, the  
217 gel was incubated with 1M Tris-HCl PH 6.8 with 50mM DTT at room temperature for  
218 20 min. The gel was horizontally placed in a new stacking gel, re-run in 15%  
219 separating gel. Finally, the gel was then transferred to nitrocellulose and blotted by  
220 the anti-proinsulin antibody. The percentage of different molecular weight  
221 complexes was quantified using ImageJ.

222

223 **2.8. BiP promoter-driven luciferase assay**

224 INS1 cells were plated into 12-well plates 1 day before transfection. The cells were  
225 triple transfected with BiP promoter firefly-luciferase reporter plasmid (kindly  
226 provided by Dr. Randy J. Kaufman at Sanford Burnham Prebys Medical Discovery  
227 Institute), CMV-driven renilla-luciferase plasmid (Promega, Madison, WI, USA), and  
228 plasmid encoding human WT or mutant proinsulin at a DNA ratio of 1:2:5,  
229 respectively. At 48 h post-transfection, cells were collected and lysed. The severity  
230 of ER stress response was measured calculating the ratio of BiP-firefly-luciferase /  
231 Renilla luciferase activity, using Dual-Glo Luciferase assay.

232

233 **2.9. Immunofluorescence and Annexin V staining**

234 Immunofluorescence was employed in INS1 cells transfected with plasmid encoding  
235 sfGFP-tagged WT or mutant proinsulin. Briefly, transfected INS1 cells monolayer  
236 grown on coverslips were fixed with 4% paraformaldehyde for 30 min at room  
237 temperature, followed by permeabilization with 2% (wt/vol) saponin (Sigma, St  
238 Louis, MO, USA) for an additional 60 min and then blocking. The cell samples were  
239 incubated with primary antibodies followed by appropriate secondary antibodies  
240 conjugated with different fluor as indicated. Immunofluorescence images were  
241 acquired by using Axio Imager M2 (ZENISS, Baden-Württemberg, Germany).

242

243 For measuring apoptotsis in beta cells expressing proinsulin mutants, INS1 cells  
244 transfected with sfGFP-tagged proinsulin were fixed, permeabilized, blocked and

245 incubated with cleaved caspase 3 antibody following the protocol described above.  
246 For surface Annexin V staining, adherent cells were incubated with Annexin V  
247 (detected by Alexa Fluor™ 555) directly at room temperature for 1 hour, followed by  
248 fixation.

249

## 250 **2.10. Statistical analysis**

251 All data were processed with GraphPad Prism 7 software and presented as means ±  
252 SD. Student's t test and ANOVA was used to determine significance between  
253 groups. A p value < 0.05 was considered as statistically significant.

254

## 255 **3. Results**

256

### 257 **3.1. Clinical characterization of three patients with *INS* variants in the B chain**

258 A previously published heterozygous *INS* gene variant, c.130G>A p.Gly44Arg  
259 [G(B20)R], was identified in two unrelated female patients (Flannick, Beer, Bick et al.,  
260 2013). One of them was diagnosed with impaired fasting glucose (IFG) at the age of  
261 17 years, without symptoms of diabetes. Currently, 18 years after the initial  
262 manifestation of diabetes, her blood glucose is well controlled [glycated hemoglobin  
263 A1c, (HbA1c), 5.4%] by diet alone. The other proband, who is now aged 33 years,  
264 was identified by an elevated HbA1c (11.0%) 4 years ago. Metformin therapy was  
265 started upon diagnosis of diabetes, and insulin injection was initiated several  
266 months ago because of pregnancy. Notably, the HbA1c decreased to 5.4% at the last

267 visit. No relatives of either patient were affected.

268

269 A novel leucine substitution for proline at the 52nd residue, c.155C>T p.Pro52Leu  
270 [P(B28)L], was identified in a 40-year-old male who suffered from polyuria and  
271 unexplained weight loss, and presented with fasting hyperglycemia and elevated  
272 HbA1c (11.8%). He was treated with metformin and the HbA1c had decreased to  
273 7.9% at the last visit, 2 years after diagnosis. The proband's father and paternal  
274 grandfather were diagnosed with diabetes prior to the age of 40 years. The clinical  
275 characteristics of the three probands are listed in Table 1.

276

### 277 **3.2. *INS* variants impair proinsulin oxidative folding and the ER export**

278 Previous research has described that *INS* gene variants commonly cause severe  
279 insulin-deficient NDM (Stoy, Edghill, Flanagan et al., 2007, Colombo, Porzio, Liu et al.,  
280 2008) and also could be a rare cause of MODY (Boesgaard, Pruhova, Andersson et  
281 al., 2010). The three patients from this study presented with relatively mild diabetes  
282 phenotypes that could be managed with diet and/or oral hypoglycemic agents.  
283 We therefore investigated the extent to which MODY-*INS* variants affected  
284 proinsulin folding, trafficking, and maturation compared with variants associated  
285 with NDM. Preproinsulin consists sequentially of the signal peptide (SP), insulin  
286 B-chain, C peptide, and insulin A-chain. Three highly conserved disulfide bonds  
287 (B19-A20, A6-A11, and B7-A7) are critical for proper folding of proinsulin in the ER  
288 (Fig. 1). Amino acid sequence alignment of proinsulin B-chains from various species

289 showed that the glycine at B20 and the proline at B28 are both highly conserved,  
290 suggesting that they may be important for proinsulin folding. To experimentally test  
291 this, we expressed WT, MODY mutants G(B20)R and P(B28)L, and NDM mutant  
292 C(A7)Y proinsulin in 293T cells. The folding of newly synthesized proinsulin was  
293 examined using tris-tricine-urea-SDS-PAGE under both reducing and non-reducing  
294 conditions (Guo et al., 2014, Liu et al., 2005). Although the total amount of newly  
295 synthesized proinsulin was comparable under reducing conditions (Fig. 2, *right*  
296 *panel*), the monomeric forms (including native, disulfide isomer, and reduced forms,  
297 Fig. 2, *left panel*) of mutant proinsulins were significantly decreased compared with  
298 that of WT-proinsulin (Fig. 2, *left panel*), suggesting that proinsulin mutants formed  
299 more mispaired disulfide isomers and disulfide-linked protein complexes that were  
300 not recovered as proinsulin monomers under non-reducing conditions.

301

302 Misfolded proteins can be recognized and retained by the ER quality control system.  
303 We therefore asked the extent to which NDM and MODY mutations impair  
304 proinsulin ER export. We used two approaches: pulse-chase radiolabeling to follow  
305 newly-synthesized proinsulin, and Western blotting to evaluate the efficiency of  
306 proinsulin secretion at steady state. We found that compared with WT-Proinsulin,  
307 the secretion of MODY or NDM mutants were dramatically decreased for both the  
308 newly synthesized (Fig. 2B-C) and steady state proinsulin (Fig. 2D-E). The  
309 hyperproinsulinemia-inducing mutation proinsulin-R65L was well secreted.  
310 Importantly, although the NDM-causing C(A7)Y mutation almost abolished

311 proinsulin secretion, up to 20% of the MODY mutations G(B20)R- or  
312 P(B28)L-proinsulin could indeed escape from the ER and be secreted from cells (Fig.  
313 2B-E). Furthermore, another MODY-inducing mutation R(B22)Q, which usually  
314 causes diabetes during adolescence (Stoy, Olsen, Park et al., 2017), showed  
315 decreased secretion compared to G(B20)R or P(B28)L. These results indicate that  
316 the severity of the proinsulin secretion defect correlates with the diabetes  
317 phenotypes associated with these *INS* mutations.

318

### 319 **3.3. Proinsulin mutants form misfolded disulfide-linked proinsulin complexes** 320 **(DLPC) in the ER**

321 As the monomeric mutant proinsulins exhibited dramatically decreased recovery  
322 under non-reducing conditions (Fig. 2A), we asked whether these mutants formed  
323 disulfide linked protein complexes. We performed Western blotting using  
324 anti-proinsulin monoclonal antibody that could detect misfolded proinsulin under  
325 nonreducing conditions (Arunagiri et al., 2019,Zhu et al., 2019), and found that the  
326 proinsulin mutants indeed formed more DLPCs (Fig. S1). To further confirm that  
327 proinsulin molecules were involved in formation of these DLPCs, we ran  
328 two-dimensional SDS-PAGE to allow intermolecular disulfide bonds present in the  
329 first dimension to be partially broken such that proinsulin monomers were released  
330 from the complexes. We found that some proinsulin molecules in the DLPCs were  
331 released as monomers in the presence of the reducing agent dithiothreitol (DTT)  
332 (Fig. S2). Next, we cut the first dimensional non-reducing gel into six pieces based



333 on the molecular weight and boiled in SDS plus 100mM DTT, and re-ran the samples.  
334 Consistent with our previous reports (Liu et al., 2012, Liu, Li, Cavener et al.,  
335 2005, Arunagiri, Haataja, Pottekat et al., 2019), we found that more than 50% of  
336 WT-proinsulin was expressed as native monomer with a molecular weight ranging  
337 from 6–14 KD, followed by about 20% expressed as HMW complexes ranging from  
338 49 to 198 KD, and < 10% WT-proinsulin expressed in the dimeric, trimeric, or  
339 tetrameric forms (Figs. 3A, E). However, C(A7)Y, G(B20)R, or P(B28)L proinsulin  
340 showed decreased monomer (< 40%) and increased dimer, trimer, tetramer, and  
341 high HMW DLPCs (Figs. 3B–E). Together, these data demonstrate that C(A7)Y,  
342 G(B20)R, and P(B28)L proinsulin were misfolded to an abnormally high degree.

343

344 **3.4. Proinsulin mutants interact with co-expressed WT-proinsulin and impair**  
345 **the ER export of WT-proinsulin.**

346 All NDM and MODY proinsulin mutants behave in a dominant fashion. We have  
347 previously shown that C(A7)Y mutant could interact with co-expressed  
348 WT-proinsulin and block its ER export (Liu, Hodish, Rhodes et al., 2007). To explore  
349 whether this dominant negative mechanism is also in play for MODY G(B20)R and  
350 P(B28)L mutants, we co-expressed Myc-tagged WT-proinsulin with untagged  
351 mutant (or WT) proinsulin in 293T cells. We found that although the mutants  
352 impaired secretion of co-expressed WT-proinsulin, a fraction of WT-proinsulin could  
353 still escape. Specifically, the dominant-negative effect of G(B20)R, P(B28)L and  
354 R(B22)Q was milder than that of C(A7)Y (Fig. 4A-B, Fig. S3). In contrast, the

355 hyperproinsulinemia-inducing mutant R65L-proinsulin did not accumulate in the ER  
356 (Fig 2D), was well secreted, and failed to block secretion of co-expressed  
357 WT-proinsulin (Fig.4A-B). We then examined physical interactions between  
358 diabetes-causing proinsulin mutants and WT-proinsulin. As shown in the Fig. 4C-D,  
359 heterodimers and heterotrimers were clearly formed between untagged  
360 WT-proinsulin and Myc-tagged mutants. Co-immunoprecipitation experiments  
361 further confirmed interactions of WT-proinsulin and mutants (Fig. E-F). Since the  
362 mutants were misfolded and retained in the ER, the recruitment of WT-proinsulin  
363 into mixed disulfide-linked dimers/complexes was likely the underlying mechanism  
364 of the secretory blockade of co-expressed WT-proinsulin.

365

366 **3.5. Mutated proinsulin impairs endogenous insulin production and induces ER**  
367 **stress, leading to apoptosis in beta cells.**

368 To further confirm that proinsulin mutants have dominant negative effects, we  
369 transfected rat insulinoma cell line (INS1E) with superfolder GFP (sfGFP)-tagged WT  
370 or mutant proinsulin and examined insulin content in the transfected cells (the cells  
371 with sfGFP signal). As expected, the endogenous insulin production of the cells  
372 transfected with sfGFP-tagged WT-proinsulin (white arrows) was comparable to that  
373 of neighboring non-transfected INS1E cells. By contrast, cells expressing  
374 sfGFP-tagged proinsulin mutants showed significantly decreased insulin production  
375 compared to non-transfected cells that served as an internal control (Fig. 5A),  
376 further confirming dominant-negative effects of the mutants.

377

378 The accumulation of misfolded proinsulin (both mutant and WT) may result in ER  
379 stress, which has been implicated in pancreatic beta cell dysfunction (Sun, Cui, He et  
380 al., 2015). We explored whether these three mutants induced ER stress using the  
381 BiP-promoter firefly luciferase assay, as previously reported (Liu et al.,  
382 2012, Tirasophon, Welihinda and Kaufman, 1998). From this, it was apparent that  
383 the NDM C(A7)Y mutant induced a greater ER stress response compared with that  
384 of MODY G(B20)R and P(B28)L mutants in beta cells (Fig. 5B).

385

386 Persistent ER stress from NDM *INS* mutants can lead to apoptosis (Colombo et al.,  
387 2008). To verify whether MODY mutant proinsulins could induce apoptosis in beta  
388 cells, cleaved caspase-3 (an early apoptosis marker) was stained in INS1E cells  
389 expressing sfGFP-tagged proinsulins. Beta cells containing the C(A7)Y mutant  
390 induced apoptosis more strongly than the MODY mutants G(B20)R and P(B28)L  
391 (Fig. 5C-D). We then assessed surface staining of annexin V, an additional apoptosis  
392 marker. As shown in Fig. 5E-F, the percentage of Annexin V positive cells increased in  
393 beta cells 3 days after transfection with mutant proinsulins, and once again,  
394 proinsulin-C(A7)Y appeared to trigger a higher level of apoptosis than either of the  
395 two MODY mutants.

396

#### 397 **4. DISCUSSION**

398

399 In this study, we studied two *INS* mutations G(B20)R and P(B28)L from patients with  
400 a MODY phenotype, in comparison to the NDM-causing C(A7)Y mutation. Our  
401 study showed that the G(B20)R, P(B28)L and C(A7)Y mutations each impaired  
402 proinsulin oxidative folding in the ER, causing proinsulin misfolding and DLPC  
403 formation, with impaired ER export (Figs. 2 and 3). Among the three mutants,  
404 C(A7)Y showed the most severe proinsulin misfolding and defect of ER export, but  
405 even the newly identified MODY mutation, P(B28)L appears to form more mispaired  
406 disulfide isomers than WT-proinsulin (Fig. 2A), suggesting that proinsulin misfolding  
407 underlies the disease in each of the three cases.

408

409 It is reported that one functional *INS* gene is sufficient to maintain normoglycemia,  
410 while in patients about 80% of all *INS* gene mutations are inherited in an autosomal  
411 dominant way (Liu, Sun, Cui et al., 2015). This strongly suggests a gain-of-toxic  
412 function from the mutant protein. Previous studies have reported that abnormal  
413 interactions between co-expressed mutant and proinsulin-WT in the ER can limit  
414 WT insulin production (Liu et al., 2012, Liu et al., 2010). In this paper, we confirmed  
415 all three mutants could form DLPC with co-expressed WT-proinsulin, which  
416 impaired intracellular trafficking of WT-proinsulin, limited mature insulin production,  
417 and induced ER stress and even cell apoptosis (Fig. 4-5). These findings extend those  
418 of previous reports (Colombo et al., 2008) to include mutations that elicit a MODY  
419 phenotype. On the one hand, we found that the NDM mutation C(A7)Y caused an  
420 almost complete blockade of co-expressed WT-proinsulin export, induced the most

421 severe ER stress and apoptosis. In contrast, the MODY mutants G(B20)R and  
422 P(B28)L partially blocked the export of co-expressed WT-proinsulin (Fig. 4) and  
423 triggered milder ER stress response and less apoptosis (Fig. 5B-F). The milder degree  
424 of cell biological defect thus appears to correlate with the MODY phenotype rather  
425 than the NDM phenotype.

426

427 To date, around half of the autosomal dominant *INS* gene mutations have been  
428 predicted and/or experimentally confirmed to affect the folding process of  
429 proinsulin in the ER (Liu et al., 2010, Liu et al., 2015, Liu, Weiss, Arunagiri et al., 2018).  
430 The most well-studied *INS* gene mutation of this type is the C(A7)Y mutation, the  
431 severity of which may be due to the availability of an unpaired B7 cysteine to form  
432 abnormal disulfide linkages with other cysteine residues. *INS* gene mutations with  
433 unpaired cysteines are prone to interfering with disulfide maturation, leading to  
434 proinsulin misfolding (Liu et al., 2010, Liu et al., 2005) (Rajpal, Schuiki, Liu et al.,  
435 2012). However, the MODY mutants studied here bear all 6 native cysteine residues.

436

437 The B chain of insulin contains a type-II' beta-turn (B7-B10) and a type-I beta-turn  
438 (B20-B23), both of which contain highly conserved glycines, including GlyB8 and  
439 GlyB20 (Weiss, 2009); folding efficiency appears to depend to a much greater extent  
440 on the dihedral angle at GlyB8 (Nakagawa, Zhao, Hua et al., 2005).] Indeed, an  
441 alanine substitution at B20 actually results in an increased affinity for the insulin  
442 receptor (Kristensen, Kjeldsen, Wiberg et al., 1997). Conceivably, G(B20)R might also

443 enhance insulin receptor binding affinity. Nevertheless, previous work has found  
444 that replacing GlyB20 (or ArgB22) with alanine produced poor yield in a yeast  
445 expression system, which may due to structure alteration of beta-turn B20–B23  
446 (Kristensen et al., 1997). Especially, GlyB20 appears to be essential for the shift from  
447 the alpha-helix B8–B19 to the beta-turn B20–B23 and maintains a positive phi  
448 dihedral angle ( “D-glycines” )(Nakagawa, Hua, Hu et al., 2006), which could be  
449 perturbed by any L-amino acid substitution.

450

451 Indeed, chain combination studies showed a reduced yield of insulin chain  
452 combination for L-AlaB20, but remarkably, yield could be rescued by chiral inversion  
453 D-AlaB20 (Nakagawa et al., 2006). This implies that the negative phi angle of  
454 G(B20)R is likely to enable folding, albeit with decreased efficiency. The G(B20)R  
455 proinsulin mutation does not directly generate any novel unpaired cysteine residues,  
456 yet structural analysis predicts it is highly possible that it might diminish the  
457 efficiency of (Cys)B19-(Cys)A20 disulfide bond formation (given that the 20th  
458 residue of the B-chain is adjacent to the disulfide bond B19-A20). Further  
459 investigation is still needed to verify if this is the case.

460

461 It should also be noted that two female probands carrying the same G(B20)R  
462 mutation showed different clinical features: one was diagnosed with mild fasting  
463 hyperglycemia controlled by diet alone, while the other presented with obviously  
464 increased HbAc1 requiring medical therapy. Indeed, a single mutation in the *INS*

465 gene can be associated with a spectrum of phenotypes even within the same family  
466 (Edghill, Flanagan, Patch et al., 2008). One example comes from a proband carrying  
467 the p.Cys43Gly [C(B19)G] mutation, which disrupts one of the conserved disulfide  
468 bonds, leading to proinsulin misfolding. The proband developed very severe  
469 diabetes at 43 weeks after birth; however his father who carried the same mutation  
470 was diagnosed with type 2 diabetes at the age of 30 years.

471

472 Another example is the NDM-causing mutation p. Gly32Ser [G(B8)S], which has also  
473 been found to cause diabetes onset at the age of ~ 3 years (Bonfanti, Colombo,  
474 Nocerino et al., 2009). Almost certainly the variation in clinical presentation  
475 depends on additional genetic and environmental factors (Stoy et al., 2007).  
476 Notably, Weiss and colleagues have reported that proinsulin-G(B8)S could lead to an  
477 insulin that has a higher-than-WT affinity to the insulin receptor, yet  
478 proinsulin-G(B8)S displays impaired folding (Avital-Shmilovici, Whittaker, Weiss et al.,  
479 2014). Altogether these findings, and our present results, highlight diabetic  
480 phenotypes initiated by impaired proinsulin folding, followed thereafter by  
481 additional downstream consequences.

482

### 483 **Funding**

484

485 This work was supported by the National Natural Science Foundation of China  
486 (81700699, 81620108004, 81830025, 81870533); the Ministry of Science and

487 Technology of China (2019YFA0802502); the Tianjin Municipal Science and  
488 Technology Bureau (17ZXMFSY00150 and 18JCYBJC93900) and The Second Hospital  
489 of Tianjin Medical University Youth Program (2017YDEY19). The work of L.H. and P.A.  
490 was supported by NIH DK48280.

491

#### 492 **Declaration of competing interest**

493

494 None.

495

#### 496 **References**

497

- 498 [1] Liu, M., Weiss, M.A., Arunagiri, A., Yong, J., Rege, N., Sun, J.H., Haataja, L., Kaufman, R.J. and  
499 Arvan, P., 2018. Biosynthesis, structure, and folding of the insulin precursor protein,  
500 *Diabetes Obesity & Metabolism*. 20, 28-50.
- 501 [2] Sun, J., Cui, J., He, Q., Chen, Z., Arvan, P. and Liu, M., 2015. Proinsulin misfolding and  
502 endoplasmic reticulum stress during the development and progression of diabetes, *Mol*  
503 *Aspects Med*. 42, 105-118.
- 504 [3] Dodson, G. and Steiner, D.F., 1998. The role of assembly in insulin's biosynthesis., *Curr Opin*  
505 *Struct Biol*. 8, 189-94.
- 506 [4] Steiner, D.F., Cunningham, D., Spigelman, L. and Aten, B., 1967. Insulin Biosynthesis:  
507 Evidence for a Precursor, *Science*. 157, 697-700.
- 508 [5] Guo, H., Xiong, Y., Witkowski, P., Cui, J., Wang, L.J., Sun, J., Lara-Lemus, R., Haataja, L.,  
509 Hutchison, K., Shan, S.O., Arvan, P. and Liu, M., 2014. Inefficient translocation of  
510 preproinsulin contributes to pancreatic beta cell failure and late-onset diabetes, *J Biol Chem*.  
511 289, 16290-302.
- 512 [6] Liu, M., Lara-Lemus, R., Shan, S.O., Wright, J., Haataja, L., Barbetti, F., Guo, H., Larkin, D. and  
513 Arvan, P., 2012. Impaired cleavage of preproinsulin signal peptide linked to  
514 autosomal-dominant diabetes, *Diabetes*. 61, 828-37.
- 515 [7] Liu, M., Li, Y., Cavener, D. and Arvan, P., 2005. Proinsulin disulfide maturation and misfolding  
516 in the endoplasmic reticulum., *J Biol Chem*. 280, 13209-12.
- 517 [8] Liu, M., Ramos-Castañeda, J. and Arvan, P., 2003. Role of the Connecting Peptide in Insulin  
518 Biosynthesis, *Journal of Biological Chemistry*. 278, 14798-14805.
- 519 [9] Schuit, F.C., In't Veld, P.A. and Pipeleers, D.G., 1988. Glucose stimulates proinsulin



520 biosynthesis by a dose-dependent recruitment of pancreatic beta cells, Proceedings of the  
521 National Academy of Sciences of the United States of America. 85, 3865-3869.

522 [10] Arunagiri, A., Haataja, L., Pottekat, A., Pamenan, F., Kim, S., Zeltser, L.M., Paton, A.W., Paton,  
523 J.C., Tsai, B., Itkin-Ansari, P., Kaufman, R.J., Liu, M. and Arvan, P., 2019. Proinsulin misfolding  
524 is an early event in the progression to type 2 diabetes, *Elife*. 8, e44532.

525 [11] Zhu, R., Li, X., Xu, J., Barrabi, C., Kekulandara, D., Woods, J., Chen, X. and Liu, M., 2019.  
526 Defective endoplasmic reticulum export causes proinsulin misfolding in pancreatic  $\beta$  cells,  
527 *Molecular and Cellular Endocrinology*. 110470.

528 [12] Jang, I., Pottekat, A., Poothong, J., Yong, J., Lagunas-Acosta, J., Charbono, A., Chen, Z.,  
529 Scheuner, D.L., Liu, M., Itkin-Ansari, P., Arvan, P. and Kaufman, R.J., 2019. PDIA1/P4HB is  
530 required for efficient proinsulin maturation and  $\beta$  cell health in response to diet induced  
531 obesity, *eLife*. 8, e44528.

532 [13] Tsuchiya, Y., Saito, M., Kadokura, H., Miyazaki, J.I., Tashiro, F., Imagawa, Y., Iwawaki, T. and  
533 Kohno, K., 2018. IRE1-XBP1 pathway regulates oxidative proinsulin folding in pancreatic beta  
534 cells, *J Cell Biol*. 217, 1287-1301.

535 [14] Zito, E., Chin, K.T., Blais, J., Harding, H.P. and Ron, D., 2010. ERO1-beta, a pancreas-specific  
536 disulfide oxidase, promotes insulin biogenesis and glucose homeostasis, *J Cell Biol*. 188,  
537 821-32.

538 [15] Li, X., Itani, O.A., Haataja, L., Dumas, K.J., Yang, J., Cha, J., Flibotte, S., Shih, H.J., Delaney, C.E.,  
539 Xu, J., Qi, L., Arvan, P., Liu, M. and Hu, P.J., 2019. Requirement for translocon-associated  
540 protein (TRAP) alpha in insulin biogenesis, *Sci Adv*. 5, eaax0292.

541 [16] Colombo, C., Porzio, O., Liu, M., Massa, O., Vasta, M., Salardi, S., Beccaria, L., Monciotti, C.,  
542 Toni, S., Pedersen, O., Hansen, T., Federici, L., Pesavento, R., Cadario, F., Federici, G., Ghirri,  
543 P., Arvan, P., Lafusco, D., Barbetti, F. and Diab, I.S.P.E., 2008. Seven mutations in the human  
544 insulin gene linked to permanent neonatal/infancy-onset diabetes mellitus, *Journal of*  
545 *Clinical Investigation*. 118, 2148-2156.

546 [17] Stoy, J., Edghill, E.L., Flanagan, S.E., Ye, H., Paz, V.P., Pluzhnikov, A., Below, J.E., Hayes, M.G.,  
547 Cox, N.J., Lipkind, G.M., Lipton, R.B., Greeley, S.A.W., Patch, A.-M., Ellard, S., Steiner, D.F.,  
548 Hattersley, A.T., Philipson, L.H., Bell, G.I. and Neonatal Diabetes International Collaborative  
549 Group, 2007. Insulin gene mutations as a cause of permanent neonatal diabetes,  
550 *Proceedings of the National Academy of Sciences*. 104, 15040-15044.

551 [18] Liu, M., Sun, J., Cui, J., Chen, W., Guo, H., Barbetti, F. and Arvan, P., 2015. INS-gene  
552 mutations: From genetics and beta cell biology to clinical disease, *Mol Aspects Med*. 42,  
553 3-18.

554 [19] Liu, M., Hodish, I., Haataja, L., Lara-Lemus, R., Rajpal, G., Wright, J. and Arvan, P., 2010.  
555 Proinsulin misfolding and diabetes: mutant INS gene-induced diabetes of youth, *Trends in*  
556 *Endocrinology & Metabolism*. 21, 652-659.

557 [20] Weiss, M.A., 2009. Proinsulin and the Genetics of Diabetes Mellitus, *J. Biol. Chem*. 284,  
558 19159-19163.

559 [21] Park, S.-Y., Ye, H., Steiner, D.F. and Bell, G.I., 2010. Mutant proinsulin proteins associated  
560 with neonatal diabetes are retained in the endoplasmic reticulum and not efficiently  
561 secreted, *Biochemical and Biophysical Research Communications*. 391, 1449-1454.

562 [22] Liu, M., Haataja, L., Wright, J., Wickramasinghe, N.P., Hua, Q.X., Phillips, N.F., Barbetti, F.,  
563 Weiss, M.A. and Arvan, P., 2010. Mutant INS-gene induced diabetes of youth: proinsulin

- 564 cysteine residues impose dominant-negative inhibition on wild-type proinsulin transport,  
565 PLoS One. 5, e13333.
- 566 [23] Polak, M., Dechaume, A., Cavé, H., Nimri, R., Crosnier, H., Sulmont, V., de Kerdanet, M.,  
567 Scharfmann, R., Lebenthal, Y., Froguel, P. and Vaxillaire, M., 2008. Heterozygous Missense  
568 Mutations in the Insulin Gene Are Linked to Permanent Diabetes Appearing in the Neonatal  
569 Period or in Early Infancy, *Diabetes*. 57, 1115-1119.
- 570 [24] Edghill, E.L., Flanagan, S.E., Patch, A.-M., Boustred, C., Parrish, A., Shields, B., Shepherd,  
571 M.H., Hussain, K., Kapoor, R.R., Malecki, M., MacDonald, M.J., Ståhl, J., Steiner, D.F.,  
572 Philipson, L.H., Bell, G.I., Hattersley, A.T. and Ellard, S., 2008. Insulin Mutation Screening in  
573 1,044 Patients With Diabetes, *Diabetes*. 57, 1034-1042.
- 574 [25] Meur, G., Simon, A., Harun, N., Virally, M., Dechaume, A.I., Bonnefond, A.I., Fetita, S.,  
575 Tarasov, A.I., Guillausseau, P.-J., Boesgaard, T.W.v., Pedersen, O., Hansen, T., Polak, M.,  
576 Gautier, J.-F.β., Froguel, P., Rutter, G.A. and Vaxillaire, M., 2010. Insulin Gene Mutations  
577 Resulting in Early-Onset Diabetes: Marked Differences in Clinical Presentation, Metabolic  
578 Status, and Pathogenic Effect Through Endoplasmic Reticulum Retention, *Diabetes*. 59,  
579 653-661.
- 580 [26] Molven, A., Ringdal, M., Nordbå, A.M., Rådler, H., Ståhl, J., Lipkind, G.M., Steiner, D.F.,  
581 Philipson, L.H., Bergmann, I., Aarskog, D., Undlien, D.E., Jøner, G., Sævik, O., Bell, G.I. and  
582 Njølstad, P.I.R., 2008. Mutations in the Insulin Gene Can Cause MODY and  
583 Autoantibody-Negative Type 1 Diabetes, *Diabetes*. 57, 1131-1135.
- 584 [27] Donath, X., Saint-Martin, C., Dubois-Laforgue, D., Rajasingham, R., Mifsud, F., Ciangura, C.,  
585 Timsit, J., Bellanne-Chantelot, C. and Monogenic Diabetes Study Group of the Societe  
586 Francophone du, D., 2019. Next-generation sequencing identifies monogenic diabetes in 16%  
587 of patients with late adolescence/adult-onset diabetes selected on a clinical basis: a  
588 cross-sectional analysis, *BMC Med*. 17, 132.
- 589 [28] Richards, S., Aziz, N., Bale, S., Bick, D., Das, S., Gastier-Foster, J., Grody, W.W., Hegde, M.,  
590 Lyon, E., Spector, E., Voelkerding, K., Rehm, H.L. and Committee, A.L.Q.A., 2015. Standards  
591 and guidelines for the interpretation of sequence variants: a joint consensus  
592 recommendation of the American College of Medical Genetics and Genomics and the  
593 Association for Molecular Pathology, *Genet Med*. 17, 405-24.
- 594 [29] Guo, H., Sun, J., Li, X., Xiong, Y., Wang, H., Shu, H., Zhu, R., Liu, Q., Huang, Y., Madley, R.,  
595 Wang, Y., Cui, J., Arvan, P. and Liu, M., 2018. Positive charge in the n-region of the signal  
596 peptide contributes to efficient post-translational translocation of small secretory  
597 preproteins, *J Biol Chem*. 293, 1899-1907.
- 598 [30] Flannick, J., Beer, N.L., Bick, A.G., Agarwala, V., Molnes, J., Gupta, N., Burt, N.P., Florez, J.C.,  
599 Meigs, J.B., Taylor, H., Lyssenko, V., Irgens, H., Fox, E., Burslem, F., Johansson, S., Brosnan,  
600 M.J., Trimmer, J.K., Newton-Cheh, C., Tuomi, T., Molven, A., Wilson, J.G., O'Donnell, C.J.,  
601 Kathiresan, S., Hirschhorn, J.N., Njølstad, P.R., Rolph, T., Seidman, J.G., Gabriel, S., Cox, D.R.,  
602 Seidman, C.E., Groop, L. and Altshuler, D., 2013. Assessing the phenotypic effects in the  
603 general population of rare variants in genes for a dominant Mendelian form of diabetes, *Nat*  
604 *Genet*. 45, 1380-5.
- 605 [31] Stoy, J., Edghill, E.L., Flanagan, S.E., Ye, H., Paz, V.P., Pluzhnikov, A., Below, J.E., Hayes, M.G.,  
606 Cox, N.J., Lipkind, G.M., Lipton, R.B., Greeley, S.A., Patch, A.M., Ellard, S., Steiner, D.F.,  
607 Hattersley, A.T., Philipson, L.H., Bell, G.I. and Neonatal Diabetes International Collaborative,

608 G., 2007. Insulin gene mutations as a cause of permanent neonatal diabetes, *Proc Natl Acad Sci U S A.* 104, 15040-4.

609

610 [32] Colombo, C., Porzio, O., Liu, M., Massa, O., Vasta, M., Salardi, S., Beccaria, L., Monciotti, C.,  
611 Toni, S., Pedersen, O., Hansen, T., Federici, L., Pesavento, R., Cadario, F., Federici, G., Ghirri,  
612 P., Arvan, P., Iafusco, D., Barbetti, F., Early Onset Diabetes Study Group of the Italian Society  
613 of Pediatric, E. and Diabetes, 2008. Seven mutations in the human insulin gene linked to  
614 permanent neonatal/infancy-onset diabetes mellitus, *J Clin Invest.* 118, 2148-56.

615 [33] Boesgaard, T.W., Pruhova, S., Andersson, E.A., Cinek, O., Obermannova, B., Lauenborg, J.,  
616 Damm, P., Bergholdt, R., Pociot, F., Pisinger, C., Barbetti, F., Lebl, J., Pedersen, O. and Hansen,  
617 T., 2010. Further evidence that mutations in INS can be a rare cause of Maturity-Onset  
618 Diabetes of the Young (MODY), *BMC Med Genet.* 11, 42.

619 [34] Stoy, J., Olsen, J., Park, S.Y., Gregersen, S., Hjørringgaard, C.U. and Bell, G.I., 2017. In vivo  
620 measurement and biological characterisation of the diabetes-associated mutant insulin  
621 p.R46Q (GlnB22-insulin), *Diabetologia.* 60, 1423-1431.

622 [35] Liu, M., Li, Y., Cavener, D. and Arvan, P., 2005. Proinsulin disulfide maturation and misfolding  
623 in the endoplasmic reticulum, *J Biol Chem.* 280, 13209-12.

624 [36] Arunagiri, A., Haataja, L., Pottekat, A., Pamenan, F., Kim, S., Zeltser, L.M., Paton, A.W., Paton,  
625 J.C., Tsai, B., Itkin-Ansari, P., Kaufman, R.J., Liu, M. and Arvan, P., 2019. Proinsulin misfolding  
626 is an early event in the progression to type 2 diabetes, *Elife.* 8.

627 [37] Liu, M., Hodish, I., Rhodes, C.J. and Arvan, P., 2007. Proinsulin maturation, misfolding, and  
628 proteotoxicity, *Proc Natl Acad Sci U S A.* 104, 15841-6.

629 [38] Sun, J., Cui, J., He, Q., Chen, Z., Arvan, P. and Liu, M., 2015. Proinsulin misfolding and  
630 endoplasmic reticulum stress during the development and progression of diabetes, *Mol*  
631 *Aspects Med.* 42, 105-18.

632 [39] Tirasophon, W., Welihinda, A.A. and Kaufman, R.J., 1998. A stress response pathway from  
633 the endoplasmic reticulum to the nucleus requires a novel bifunctional protein  
634 kinase/endoribonuclease (Ire1p) in mammalian cells, *Genes & Development.* 12,  
635 1812-1824.

636 [40] Liu, M., Sun, J., Cui, J., Chen, W., Guo, H., Barbetti, F. and Arvan, P., 2015. INS-gene  
637 mutations: from genetics and beta cell biology to clinical disease, *Mol Aspects Med.* 42,  
638 3-18.

639 [41] Liu, M., Weiss, M.A., Arunagiri, A., Yong, J., Rege, N., Sun, J., Haataja, L., Kaufman, R.J. and  
640 Arvan, P., 2018. Biosynthesis, structure, and folding of the insulin precursor protein,  
641 *Diabetes Obes Metab.* 20 Suppl 2, 28-50.

642 [42] Rajpal, G., Schuiki, I., Liu, M., Volchuk, A. and Arvan, P., 2012. Action of protein disulfide  
643 isomerase on proinsulin exit from endoplasmic reticulum of pancreatic beta-cells, *J Biol*  
644 *Chem.* 287, 43-7.

645 [43] Weiss, M.A., 2009. The structure and function of insulin: decoding the TR transition, *Vitam*  
646 *Horm.* 80, 33-49.

647 [44] Nakagawa, S.H., Zhao, M., Hua, Q.X., Hu, S.Q., Wan, Z.L., Jia, W. and Weiss, M.A., 2005.  
648 Chiral mutagenesis of insulin. Foldability and function are inversely regulated by a  
649 stereospecific switch in the B chain, *Biochemistry.* 44, 4984-99.

650 [45] Kristensen, C., Kjeldsen, T., Wiberg, F.C., Schaffer, L., Hach, M., Havelund, S., Bass, J., Steiner,  
651 D.F. and Andersen, A.S., 1997. Alanine scanning mutagenesis of insulin, *J Biol Chem.* 272,

652 12978-83.

653 [46] Nakagawa, S.H., Hua, Q.X., Hu, S.Q., Jia, W., Wang, S., Katsoyannis, P.G. and Weiss, M.A.,  
654 2006. Chiral mutagenesis of insulin. Contribution of the B20-B23 beta-turn to activity and  
655 stability, *J Biol Chem.* 281, 22386-96.

656 [47] Edghill, E.L., Flanagan, S.E., Patch, A.M., Boustred, C., Parrish, A., Shields, B., Shepherd, M.H.,  
657 Hussain, K., Kapoor, R.R., Malecki, M., MacDonald, M.J., Stoy, J., Steiner, D.F., Philipson, L.H.,  
658 Bell, G.I., Neonatal Diabetes International Collaborative, G., Hattersley, A.T. and Ellard, S.,  
659 2008. Insulin mutation screening in 1,044 patients with diabetes: mutations in the INS gene  
660 are a common cause of neonatal diabetes but a rare cause of diabetes diagnosed in  
661 childhood or adulthood, *Diabetes.* 57, 1034-42.

662 [48] Bonfanti, R., Colombo, C., Nocerino, V., Massa, O., Lampasona, V., Iafusco, D., Viscardi, M.,  
663 Chiumello, G., Meschi, F. and Barbetti, F., 2009. Insulin gene mutations as cause of diabetes  
664 in children negative for five type 1 diabetes autoantibodies, *Diabetes Care.* 32, 123-5.

665 [49] Avital-Shmilovici, M., Whittaker, J., Weiss, M.A. and Kent, S.B., 2014. Deciphering a  
666 molecular mechanism of neonatal diabetes mellitus by the chemical synthesis of a protein  
667 diastereomer, [D-AlaB8]human proinsulin, *J Biol Chem.* 289, 23683-92.

668

669

670

671

672

673

674

675

676

677

678

679

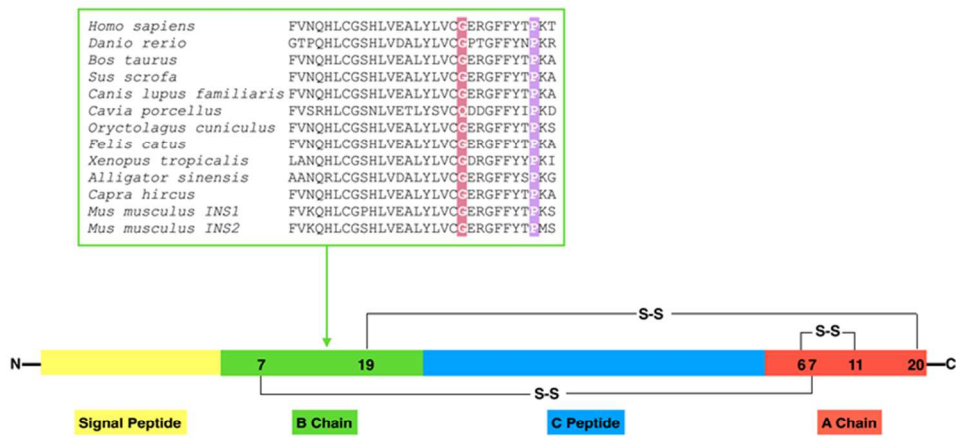
680

681

682

683 **Figures and Figure legends**

**Fig.1**



684

685 **Fig. 1. Highly conserved amino acids B20 and B28 in different species.** Structure of  
 686 preproinsulin: The signal peptide (SP, yellow), insulin B chain (green), C peptide  
 687 (blue), insulin A chain (red), S-S indicate the B19-A20, A6-A11, B7-A7 three different  
 688 disulfide bonds. B chain alignment between human *INS* and orthologs. Amino acids  
 689 B20 and B28 were marked with red and purple, respectively.

690

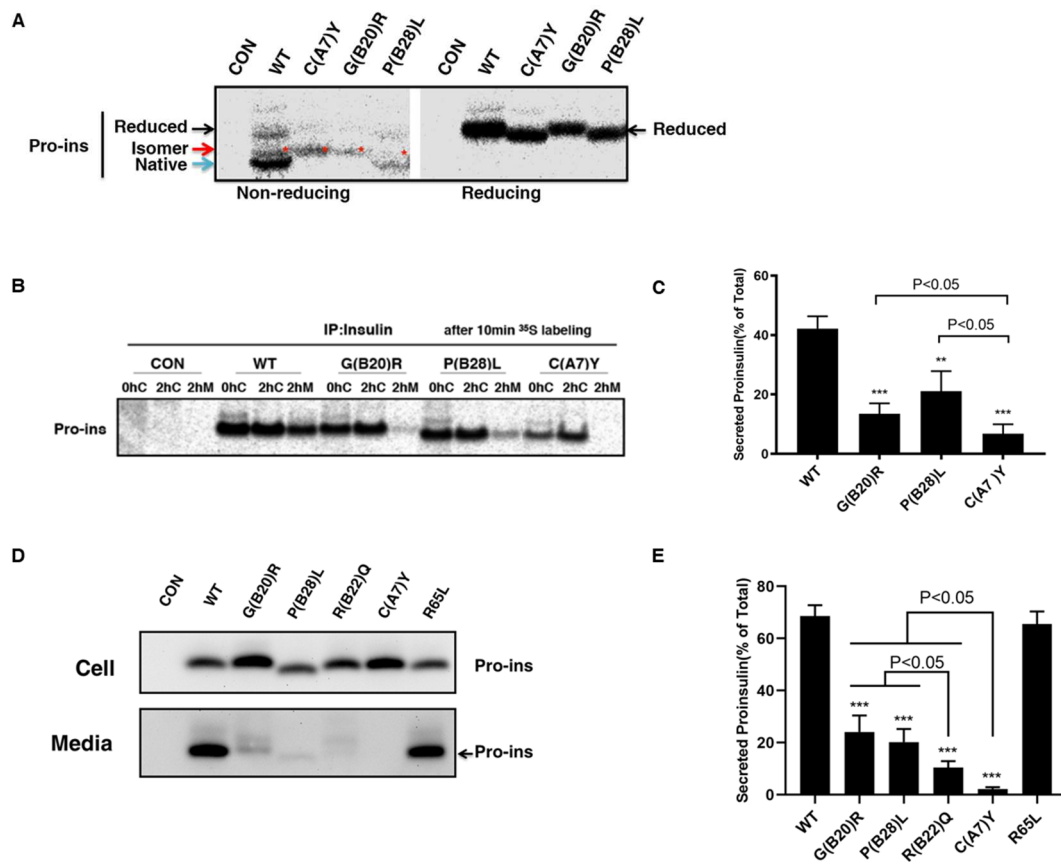
691

692

693

694

Fig.2



696

697 **Fig. 2. *INS* variants impair proinsulin oxidative folding and ER export.** A. 293T cells  
 698 were transfected with plasmids encoding wild-type (WT), or mutants C(A7)Y,  
 699 G(B20)R, P(B28)L. At 48 h post-transfection, the cells were labeled with <sup>35</sup>S-Met/Cys  
 700 for 10 min. The newly synthesized proinsulin were precipitated with anti-insulin and  
 701 analyzed by Tris–tricine–urea–SDS-PAGE under both non-reducing or reducing  
 702 conditions. Reduced forms proinsulin marked by the black arrow, native forms  
 703 marked by the blue arrow, disulfide isomers marked by the red arrow and star. B.  
 704 293T cells were transfected as Fig. 2A and pulse-labeled at 48 h with <sup>35</sup>S-Met/Cys for  
 705 10 min followed by 0 or 2 h chase. Both cell lysates harvested after 0h (0hC) or 2h  
 706 (2hC) chase and chase media (2hM) were immunoprecipitated with the anti-insulin

707 and analyzed in 4-12% NuPage gel under reducing conditions with autoradiography.

708 **C.** The secretion efficiency of WT or mutant proinsulin from at least three

709 independent experiments shown in Fig. 2B was quantified using ImageJ. The results

710 were shown as mean±SD, \*\* p <0.01 and \*\*\* p <0.001 comparing to WT (ANOVA

711 test). **D.** 293T cells were transfected with plasmids encoding WT or mutant

712 proinsulin as indicated. At 24 h post-transfection, the culture media were changed.

713 After additional 24 hour incubation, the media were collected and cells were lysed.

714 Both media and lysates were subjected to western blotting using anti-proinsulin

715 antibody. **E.** The secretion efficiency of WT or mutant proinsulin under steady state

716 from at least three independent experiments shown in Fig. 2D was quantified using

717 ImageJ. The results were shown as mean±SD, \*\*\* p <0.001 comparing to WT

718 (ANOVA test).

719

720

721

722

723

724

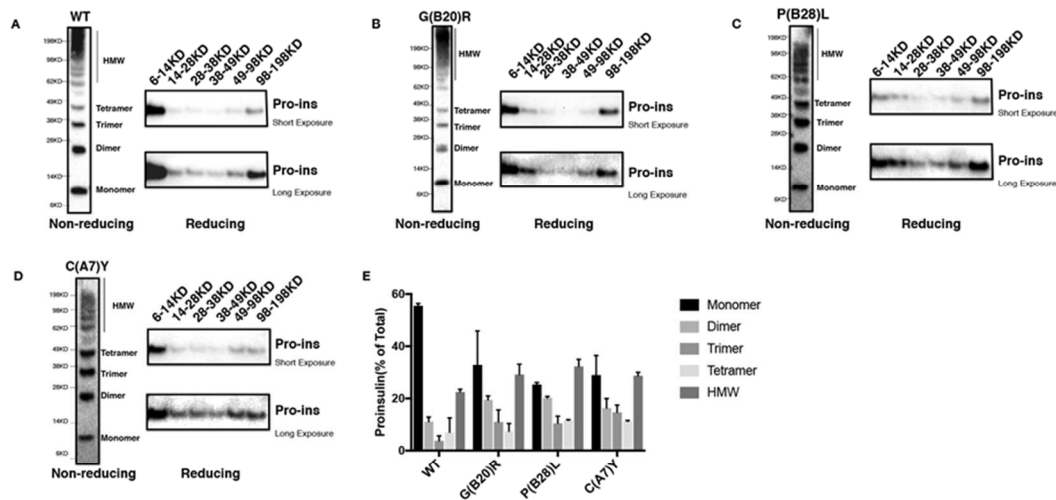
725

726

727

728

Fig.3



729

730 **Fig. 3. Proinsulin mutants form misfolded disulfide-linked proinsulin complexes**

731 **(DLPC) in the ER.** 293T cells were transfected with Myc-tagged plasmids encoding

732 WT or mutant proinsulin. At 48 h post-transfection, cell lysates were resolved in

733 4-12% NuPage under non-reducing condition (left panel). The gels were cut into 6

734 pieces corresponding to the molecular weight, then boiled in the sample buffer

735 containing 100mM DTT followed by resolved again in 4-12% NuPage. The gels were

736 transferred to nitrocellulose following by blotting with anti-proinsulin antibody. The

737 same procedure was processed both for WT **(A)**, G(B20)R **(B)**, P(B28)L **(C)**, and

738 C(A7)Y **(D)**. **E.** The 2-DE assay shown in Fig. 3A-D from at least three independent

739 experiments was quantified using ImageJ. The percentages of fully reduced

740 proinsulin monomer(6-14KD), dimer(14-28KD), trimer(28-38KD), tetramer(38-49KD)

741 and high molecular weight (HMW) complexes (49-198KD) in total proinsulin



742 molecules were calculated and shown as mean±SD.

743

744

745

746

747

748

749

750

751

752

753

754

755

756

757

758

759

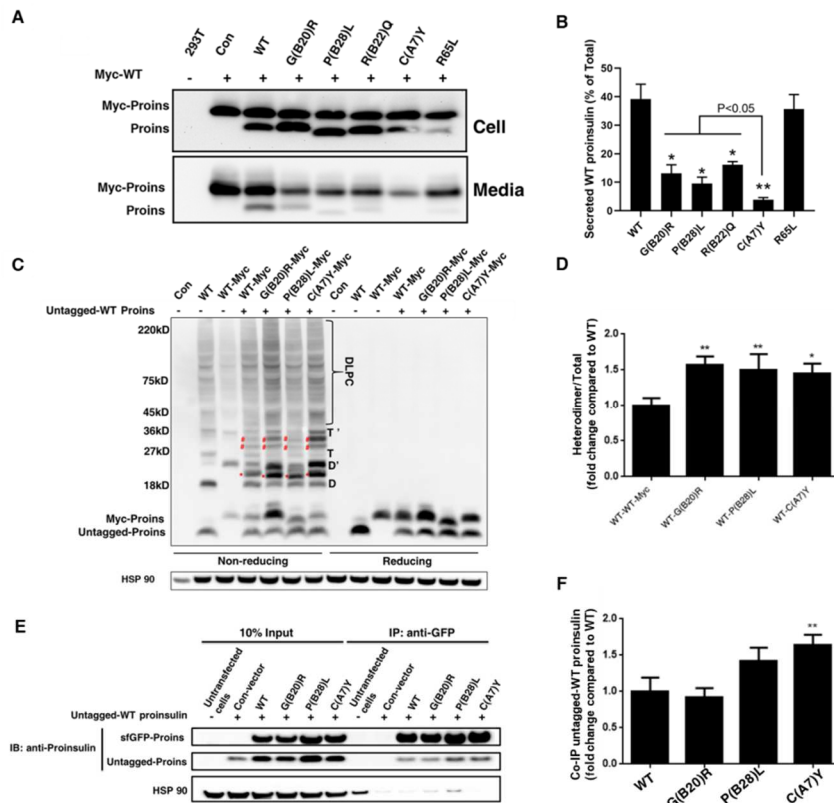
760

761

762

763

Fig.4



764

765 **Fig.4. Proinsulin mutants interact with co-expressed WT-proinsulin and impair the**  
 766 **ER export of WT-proinsulin.**

767 **A-B.** 293T cells were co-transfected with Myc-tagged WT-proinsulin (upper bands)  
 768 and untagged WT-proinsulin or mutants (lower bands) as indicated. The secretion of  
 769 Myc-tagged WT-proinsulin in the presence of untagged WT-proinsulin or mutants  
 770 under 24h steady state was examined by immuno-blotting using anti-proinsulin. The  
 771 percentages of secreted WT-proinsulin were quantified and calculated. \* p <0.05  
 772 and \*\* p <0.01 comparing to WT (ANOVA test). **C-D.** 293T cells were co-transfected  
 773 with untagged WT-proinsulin and Myc-tagged WT-proinsulin or mutants. The  
 774 monomers, dimers (D refers to homodimers formed by untagged Proins, and D'  
 775 refers to homodimers formed by Myc-Proins, red star refers to heterodimers formed  
 776 by untagged Proins and Myc-Proins), trimers (T refers to homotrimers formed by

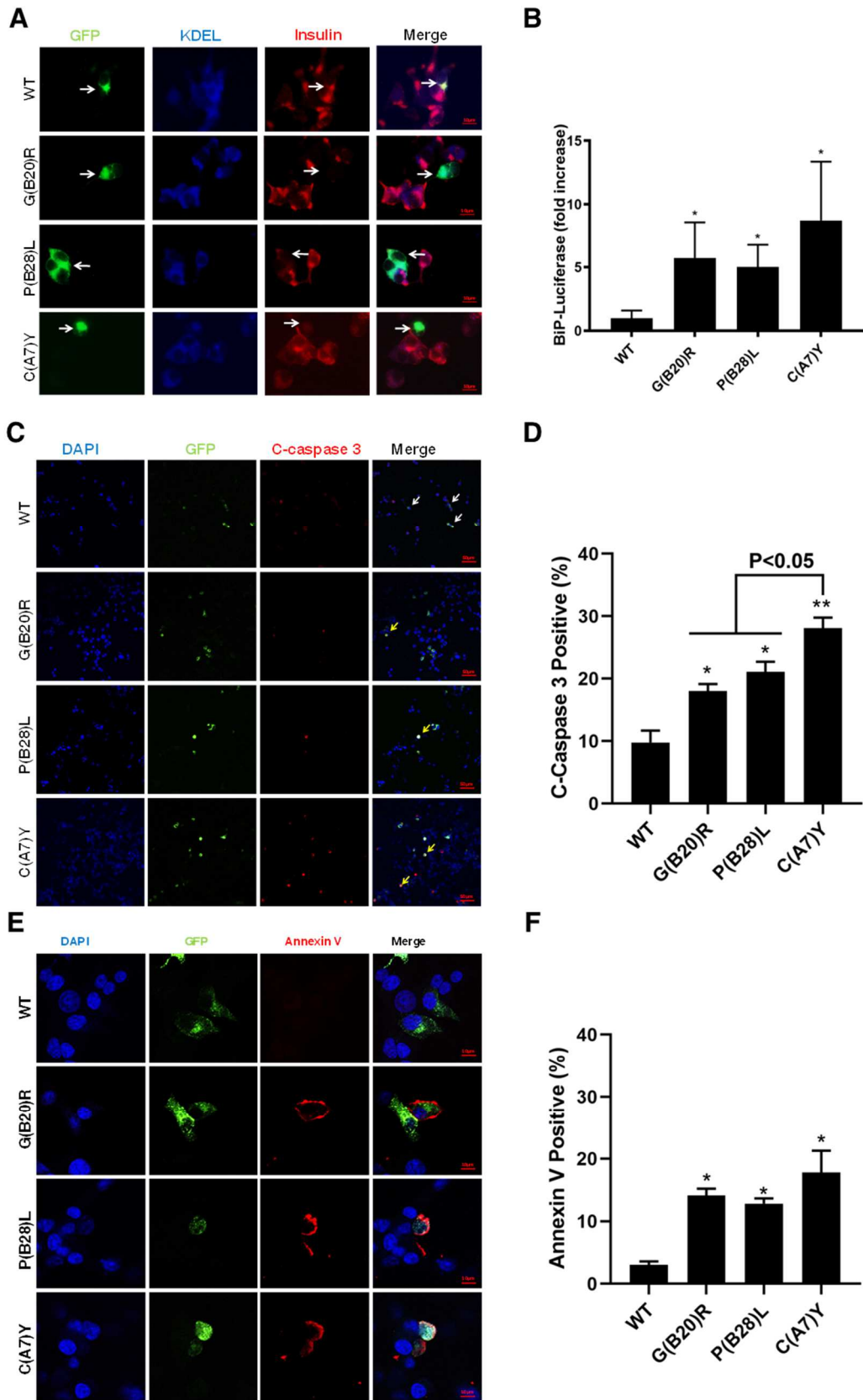
777 untagged Proins, and T' refers to homotrimers formed by Myc-Proins, blue star  
778 refers to heterotrimers formed by untagged Proins and Myc-Proins), and  
779 higher-molecular weight disulfide-linked proinsulin complexes (DLPC) were analyzed  
780 under non reducing conditions. The total amount of untagged WT-proinsulin and  
781 Myc-tagged WT or mutants were analyzed under reducing condition. The  
782 percentages of heterodimer (red star marked) formed by untagged WT Proins and  
783 Myc-tagged proinsulin mutant were calculated. The percentage of heterodimer  
784 formed by untagged Proins-WT and Myc tagged Proins-WT was set to 1. \*  $p < 0.05$   
785 and \*\*  $p < 0.01$  comparing to WT (ANOVA test). **E-F.** 293T cells were co-transfected  
786 with untagged WT-proinsulin and super folder (sf) GFP-tagged WT-proinsulin or  
787 mutants. At 48 h post-transfection, cells were lysed and immunoprecipitated with  
788 the anti-GFP antibody, followed by immuno-blotting (IB) with anti-proinsulin  
789 antibody. The percentages of untagged WT-proinsulin pulled down by sfGFP-tagged  
790 proinsulin-WT or mutants were quantified and calculated. \*\*  $p < 0.01$  comparing  
791 to WT (ANOVA test).

792

793

794

**Fig.5**



795

796 **Fig.5. Proinsulin mutants decrease endogenous insulin production and induce ER**

797 **stress, leading to apoptosis in beta cells.**

798 **A.** INS1 cells were transfected with plasmid encoding sfGFP-tagged WT, G(B20)R,  
799 P(B28)L or C(A7)Y proinsulin. At 48h post-transfection, the cells were permeabilized  
800 and immunoblotted with anti-insulin (red) and anti-KDEL (blue, ER marker). Arrows  
801 indicate the cells expressed exogenous sfGFP-tagged WT-proinsulin or mutants.

802 **B.** INS1 cells were transiently triple-transfected with the plasmids encoding BiP  
803 promoter-firefly luciferase, CMV-driven Renilla luciferase, and WT or mutant  
804 proinsulin at ratio 1 : 2 : 5 (This ratio helps ensure that BiP-luciferase serves as a  
805 reporter from cells synthesizing exogenously expressed proinsulins). At 48 h  
806 post-transfection, the cells were lysed and a ratio of firefly/renilla luciferase was  
807 measured. The relative activities of the BiP promoter in cells expressing proinsulin  
808 mutants were compared to that in cells expressing WT-proinsulin, which served as a  
809 control and set to 1. Results are from at least three independent experiments. \*p  
810 <0.05 compared with WT-proinsulin (Student's t-test).

**C.** INS1 cells were transfected  
811 with sfGFP-tagged WT-proinsulin and variants as indicated. After 3 days post  
812 transfection, cells were fixed and stained with anti-cleaved caspase 3 antibody.  
813 Arrows indicate cells expressed exogenous proinsulin with (yellow arrow) or without  
814 (white arrow) apoptosis. **D.** Percentages of cleaved caspase 3 positive cell in

815 transfected INS1 cells were quantified. \* p <0.05 and \*\* p <0.01 comparing to WT  
816 (Student's t-test). **E.** Representative images of INS1 cells expressing sfGFP-tagged

817 proinsulin stained with Annexin V (red) and DAPI (blue) were shown. **F.** Proportion  
818 of Annexin V positive cells were quantitative analyzed. \*p <0.05 compared with

819 WT-proinsulin (Student's t-test)

820

821

822

823

824

825

826

827

828

829

830

831

832

833

834

835

836

837

838

839

840

841 **Table****Table 1. Clinical characterization of the three patients with *INS* variants in the B chain**

		Patient 1	Patient 2	Patient 3
Gender		Female	Female	Male
At diagnosis	Age (y)	17	29	40
	BMI (kg/m <sup>2</sup> )	21.3	22.3	22.7
	Fasting glycemia (mmol/l)	6.44	ND	8.91
	HbA1C (% - mmol/mol)	5.5 - 37	11 - 97	11.8 - 105
	Symptoms of diabetes	No	No	Polyuria, weight loss
	Treatment	Diet	Metformin	Metformin
	Family history	None	None	3 affected generations
Last visit	Age (y)	35	33	42
	HbA1C (% - mmol/mol)	5.4 - 36	5.4 - 36	7.9 - 63
	Treatment	Diet	Insulin (pregnancy)	Metformin
	Arterial hypertension	No	ND	No
	Dyslipidemia	No	ND	No
INS gene mutation	nuc.	c.130G>A	c.130G>A	c.155C>T
	prot.	p.Gly44Arg G(B20)R	p.Gly44Arg G(B20)R	p.Pro52Leu P(B28)L

ND: Not Determined

842

843 **Table 1. Clinical characterization of the three patients with *INS* variants in the B**  
844 **chain.**

845

846

847